arXiv:cond-mat/0007295v1 18 Jul 2000

Multiphase segregation and metal-insulator transition in single crystal $La_{5/8-y}Pr_yCa_{3/8}MnO_3$

V. Kiryukhin, B. G. Kim, V. Podzorov, S-W. Cheong
Department of Physics and Astronomy, Rutgers University, Piscataway, New Jersey 08854

T. Y. Koo
Bell Laboratories, Lucent Technologies, Murray Hill, New Jersey 07974

J. P. Hill
Department of Physics, Brookhaven National Laboratory, Upton, New York 11973

I. Moon, Y. H. Jeong
Department of Physics, Pohang University of Science and Technology, Pohang, Kyungbuk, 790-784, South Korea
(February 1, 2008)

The insulator-metal transition in single crystal $La_{5/8-y}Pr_yCa_{3/8}MnO_3$ with $y \approx 0.35$ was studied using synchrotron x-ray diffraction, electric resistivity, magnetic susceptibility, and specific heat measurements. Despite the dramatic drop in the resistivity at the insulator-metal transition temperature T_{MI}, the charge-ordering (CO) peaks exhibit no anomaly at this temperature and continue to *grow* below T_{MI}. Our data suggest then, that in addition to the CO phase, another insulating phase is present below T_{CO}. In this picture, the insulator-metal transition is due to the changes that occur *within* this latter phase. The CO phase does not appear to play a major role in this transition. We propose that a percolation-like insulator-metal transition occurs via the growth of ferromagnetic metallic domains within the parts of the sample that do not exhibit charge ordering. Finally, we find that the low-temperature phase-separated state is unstable against x-ray irradiation, which destroys the CO phase at low temperatures.

PACS numbers: 75.30.Vn, 71.30.+h, 78.70.Ck, 72.40.+w

I. INTRODUCTION

Metal-insulator transitions in manganite perovskites have attracted considerable attention during the last five years [1]. It has been established that the metallic state in these materials is ferromagnetic (with the double exchange mechanism responsible for the ferromagnetism), and a variety of insulating states have been found. In many cases, application of a magnetic field converts the insulating phase into the ferromagnetic metallic (FM) state, resulting in the phenomenon of "colossal magnetoresistance" (CMR). Recently, it has been demonstrated that microscopic phase separation plays an essential role in the physics of the manganites [2–5]. In particular, it results in the apparent percolative character of the insulator-metal transition when the transition is from the charge-ordered insulating to the ferromagnetic metallic state. It is here that the largest changes in resistivity (more than 6 orders of magnitude), and therefore the largest magnetoresistances are observed.

In spite of the large amount of work devoted to the manganites, the microscopic nature of the phase-separated states has thus far not been understood. For example, the electronic properties of the constituent phases as well as their volume fractions and spatial distributions in the sample remain to be characterized. More importantly, the physical mechanism underlying the phase separation phenomenon remains unclear. It has been proposed theoretically that doped Mott insulators, such as the mixed-valence manganites, are unstable against electronic phase separation into carrier-rich and carrier-poor regions [6]. This scenario, however, is inconsistent with the sub-μm domain size observed experimentally in several manganite materials [2]. More generally, it is unclear how such a large-scale phase separation can be ascribed to the effects of short-range local interactions or be consistent with long range Coulomb forces, and therefore other effects, including lattice strain [7] or quenched disorder [8], for instance, need to be considered. To address these basic questions and to understand the origin of the CMR effect, the microscopic structure of manganites must be characterized in detail, and, evidently, more experimental work is needed.

In this paper, we report synchrotron x-ray diffraction, electrical resistivity, magnetization, and specific heat measurements performed on single crystal samples of $La_{5/8-y}Pr_yCa_{3/8}MnO_3$, $y \approx 0.35$. With decreasing temperature, this material first undergoes a charge-ordering (CO) transition at $T_{CO} \approx 200$ K, and then a relatively sharp insulator-metal transition into a low-temperature conducting phase at $T_{MI} \approx 70$ K. This low-temperature phase is believed to consist of a mixture of charge-ordered

insulating and ferromagnetic metallic phases [2]. We estimated that the low-temperature volume fraction of the ferromagnetic phase was 30% in this sample. Note that the charge ordering is of the simple checker-board type found in the "x=0.5" samples and therefore cannot be complete in the entire sample at this doping. We find that neither the fraction of the CO phase in the sample, nor the correlation length of the CO phase, show measurable anomalies at T_{MI}. Moreover, the intensities of the CO diffraction peaks continue to grow as the temperature is decreased across the insulator-metal transition. Thus, these data show that the volume fraction of the CO phase does not decrease, and in all likelihood continues to increase, as the material undergoes the insulator-metal transition. Our combined data therefore indicate that in addition to the CO phase, another paramagnetic insulating phase is present below T_{CO}. The insulator-metal transition is then caused by the changes *within* this latter phase.

Existing experimental data suggest that the insulator-metal transition has a percolative character. We propose here that it occurs via the growth of ferromagnetic metallic domains within the parts of the sample that do not exhibit charge ordering. In this picture there are at least three phases in our samples below T_{CO}: ferromagnetic metallic, charge-ordered insulating, and a second insulating state which is paramagnetic above T_{MI}, and which we will refer to as the I2 phase (insulating phase 2). The mechanism of the metal-insulator transition in charge-ordered manganites, therefore, appears to be more complex than a simple percolation of metallic phase due to the growth of ferromagnetic domains in the charge-ordered matrix.

In addition, we have studied the volume fraction of the FM phase in several other samples with $y \approx 0.35$. The very low volume fractions of the FM phase observed in some cases indicate that the FM phase is of a filamentary character even at the lowest temperatures. We argue therefore that crystallographic or magnetic domain boundaries, lattice defects and associated strains may play an important role in the formation of the conducting state in these materials.

Finally, we have investigated the effects of x-ray irradiation on the low-temperature phase-separated state. As was the case in some other charge-ordered manganites [9–11], the CO state in our samples is destroyed by x-ray irradiation below T=50 K. The photoinduced transition was previously found to be of the insulator-metal type in related samples [9]. While the CO phase remains unaffected by the photoinduced insulator-metal transition at temperatures larger than T_{MI} in the related (Pr,Ca,Sr)MnO_3 samples [3], the CO phase in the present case is destroyed by x-rays at low temperatures. Thus, while an additional phase is required to explain the insulator-metal transition at T_{MI}, the low-temperature photoinduced transition need only involve the FM and the CO phases.

II. EXPERIMENT

Single crystals of $La_{5/8-y}Pr_yCa_{3/8}MnO_3$ were grown using the floating zone technique from polycrystalline rods with a nominal composition near y=0.35 synthesized by a standard solid state reaction method. Resistivity measurements were performed using a standard four-probe method, magnetization measurements were carried out with a commercial SQUID magnetometer, and specific heat measurements were performed using a recently developed Peltier microcalorimeter [12].

The x-ray diffraction measurements were carried out at beamline X22A at the National Synchrotron Light Source. The 10.35 keV x-ray beam was focused by a mirror, monochromatized by a Si (111) monochromator, scattered from the sample mounted inside a closed-cycle cryostat, and analyzed with a Ge (111) crystal. The x-ray beam was $\sim$0.5$\times$1 mm in cross section, and the x-ray flux was $\sim 10^{11}$ photons per second. The typical mosaic spread in our samples was 0.2°.

Below the charge-ordering transition temperature T_{CO}, superlattice diffraction peaks of two types appear. The (H, K/2, L) peaks, K odd (in the orthorhombic *Pbnm* notation), are associated with the Jahn-Teller distortions characteristic of the CE-type charge and orbitally ordered state, and are often referred to as orbital-ordering peaks. The (H, 0, 0) and (0, K, 0) peaks, H and K odd, have the same wavevector as the checker-board charge ordering and arise from lattice distortions associated with valence ordering. In a recent series of experiments [13], these reflections were studied in the related material $Pr_{1-x}Ca_xMnO_3$ which also exhibits the CE-type CO state. By tuning the incident x-ray energy through the Mn absorption edge, characteristic resonance and polarization dependences were observed at these reflections, directly confirming their assignment as orbital and charge-ordering peaks. In our measurements the x-ray energy is far from resonance, and therefore both types of superlattice reflections arise from lattice distortions associated with the CO state. In this work, we concentrated on the (0, 4.5, 0), (0, 5, 0), and (0, 5.5, 0) peaks. Longitudinal (parallel to the scattering vector) and transverse scans were taken. The longitudinal scans were fitted using Lorentzian-squared line shapes, and these fits were used to extract the intensities, positions, and widths of the peaks.

III. RESULTS AND DISCUSSION

Fig. 1 shows the temperature dependences of the zero-field electric resistivity and magnetization in a 100 Oe magnetic field. The anomalies at $T_{CO} \approx 200$ K are due

to the CO transition. With decreasing temperature, a relatively sharp insulator-metal transition occurs at T_{MI} ≈70 K. (The transition temperatures were defined as the temperatures of the maxima in the temperature derivative of the logarithmic resistivity.) In the vicinity of T_{MI}, the sample magnetization gradually increases on cooling before saturating below T=40 K. The transition is strongly hysteretic.

In a recent work by Uehara *et al.* [2] it was shown that the low-temperature state of this material is inhomogeneous, and that even at very low temperatures only a fraction of the sample becomes metallic. Assuming that these metallic parts of the sample are also ferromagnetic, this fraction can be estimated using the data of Fig. 2, which shows the sample magnetization versus applied magnetic field in a zero-field cooled sample. The magnetization first saturates at a field of about 1 Tesla. This saturation is attributed to the complete alignment of the FM domains present in the sample in zero field [2]. The material then undergoes two field-induced transitions at the fields of 1.6 and 3 Tesla. Finally, when the field is increased to H=4 Tesla the entire sample becomes ferromagnetic, as indicated by the magnitude of the saturated magnetic moment. The field-induced transition is persistent, and the entire sample remains in the FM state after the field is turned off. Therefore, the fraction of the FM state in the zero-field cooled sample can be determined from the ratio of the low-field (H<1 Tesla) magnetization taken on ramping the field up and down. Using the data of Figs. 1 and 2, we thus conclude that the fraction of the FM phase in our sample was ∼30% at T=5 K and ∼9% at T=70 K, the insulator-metal transition temperature.

One possible scenario for the insulator-metal transition in $La_{5/8-y}Pr_yCa_{3/8}MnO_3$ involves the growth of the metallic domains within the charge-ordered insulating matrix with decreasing temperature. The system would then undergo the insulator-metal transition when these metallic domains percolated. As discussed above, the volume fraction of the conducting phase can be estimated from the magnetization measurements, and in our samples should thus increase from approximately zero to ∼30% as the temperature decreases from 100 K to 40 K.

To test this hypothesis, we investigated the properties of the CO state using synchrotron x-ray diffraction. The temperature dependences of the intensity, width, and the scattering vector of the (0, 4.5, 0) superlattice peak are shown in Fig. 3. The data were taken on cooling. The intensity of this peak is often taken as the order parameter of the CE-type charge and orbital ordered state because it reflects the degree of the order achieved in the CO system provided that the sample is homogeneous. In an inhomogeneous system, this intensity can also increase if the volume fraction of the CO phase increases. Therefore, if the conducting phase grows at the expense of the CO phase as the temperature is decreased, one would expect the CO peak intensity to decrease as the sample undergoes the insulator-metal transition. In principle, it is possible that the increase in the peak intensity due to the improved ordering at low temperatures might compensate for any decrease in the volume fraction of the CO phase. However, taking into account the high volume fraction (30%) of the ferromagnetic phase at low temperatures and noting that the order parameter of the CO phase is not expected to change rapidly at temperatures much smaller than T_{CO}, we believe that the latter possibility is very unlikely [14]. That is, if 30% of the CO phase were to be transformed, we would be able to observe it. It is surprising therefore that the data of Fig. 3(a) do not show any decrease in the (0, 4.5, 0) peak intensity in the vicinity of the insulator-metal transition. On the contrary, the peak intensity continues to increase with decreasing temperature down to T=10 K, showing no detectable anomaly at T_{MI}. The intensity of the (0, 5, 0) CO peak also does not show any decrease in the vicinity of T_{MI}. We therefore conclude that our data are inconsistent with any model in which the insulator-metal transition is due to the simple growth of the FM phase at the expense of the CO phase at low temperatures.

Panel (b) of Fig. 3 shows the temperature dependence of the (0, 4.5, 0) peak width. The intrinsic peak width is inversely proportional to the correlation length of the CE-type ordered state. The data of Fig. 3b show that the correlation length of the orbital state remains finite well below the CO transition temperature, slowly growing with decreasing temperature. Even at 10 degrees below T_{CO}, it does not exceed 200 Å. It is unclear to what extent these data reflect the size of the CO domains, however, since similar peak broadening of orbital reflections was observed in $Pr_{0.5}Ca_{0.5}MnO_3$ samples in which CO reflections exhibit long range order [13]. In any case, it is evident that the orbital state is highly disordered in the vicinity of T_{CO} but becomes progressively better correlated as the temperature decreases. The CO domain size may also grow in the process. However, as was the case for the peak intensity, there is no anomaly in the temperature dependence of the peak width in the vicinity of T_{MI}, and, clearly, there is no low-temperature width increase that might be expected if charge ordering is destroyed in a third of the sample volume.

The temperature dependence of the (0, 4.5, 0) peak position is shown in Fig. 3(c). There is an abrupt change in this temperature dependence at T=200 K. This change is almost certainly caused by the structural transition. The increase in the CO scattering vector above T=200 K may be caused by the corresponding decrease in the *b*-axis lattice constant, if the CO fluctuations simply follow the underlying crystal lattice. However, more interesting explanations, including the possibility of incommensurate orbital fluctuations that were previously observed in other manganites [15], are also possible.

We have also studied the temperature-dependent be-

havior of the fundamental Bragg peaks. In particular, scattering in the vicinity of the (0, 4, 0) position in the reciprocal space was measured, and the results are shown in Fig. 4. Note that due to the presence of twin domains, (0, 4, 0), (4, 0, 0), and (2, 2, 4) reflections may, in principle, be present at this reciprocal space position. Similar to many other charge-ordered manganites, our sample undergoes a structural transition at T_{CO}. Above T=220 K a single narrow peak is observed, while below T=180 K two overlapping peaks are present (see Fig. 8 for an example of the low-temperature peak profile). It was impossible to distinguish between a single broad peak or closely separated two peaks in the vicinity of T_{CO}. Below T_{CO}, peak positions and widths evolve in a smooth manner down to T=10 K. There appears to be a small but systematic narrowing of the Bragg peaks with decreasing temperature below T_{CO}. This decrease in the peak width indicates that lattice strain is relieved as the temperature is decreased. The lattice strain is maximized in the vicinity of T_{CO}. Note that some of the decrease of the (0, 4.5, 0) peak width at low temperatures (Fig. 3(b)) may thus be attributed to the decrease of the overall lattice strain.

The temperature dependence of the specific heat is shown in Fig. 5. The temperature anomaly at T=210 K is due to the charge-ordering transition [17]. The anomaly at T=170 K is likely the result of the Néel transition which takes place in $Pr_{1-x}Ca_xMnO_3$ samples at a similar temperature [16]. As was the case for the diffraction data, the specific heat exhibits no anomaly at T_{MI}. This behavior is consistent with the multiphase scenario for the insulator-metal transition in our sample and is clearly different from the behavior exhibited by $La_{0.7}Ca_{0.3}MnO_3$. The latter compound has approximately the same doping level and exhibits a conventional metal-insulator transition at the Curie temperature at which a pronounced specific heat anomaly is observed [18].

The combined data discussed above are clearly incompatible with the picture in which the FM phase appears at a temperature of approximately 100 K, as the magnetization data would suggest, and then grows at the expense of the CO phase as the temperature decreases, percolating at T_{MI}=70 K and finally reaching a volume fraction of 30% at T=40 K. On the contrary, the temperature dependences of Fig. 3 indicate that the correlation length, and possibly even the volume fraction of the CO phase, grow with decreasing temperature.

Based on our data, we therefore propose the following modified scenario for the insulator-metal transition in $La_{5/8-y}Pr_yCa_{3/8}MnO_3$. A secondary phase (the insulating phase 2, or the I2 phase), which is distinct from the phase that undergoes the CO transition, is present in our samples below T_{CO}. Since the CO phase is insulating and its volume fraction is not decreasing with decreasing temperature, the changes *within* this secondary phase must account for the insulator-metal transition. That is, the insulator-metal transition results from the growth of ferromagnetic metallic domains within the parts of the sample that do *not* exhibit charge ordering.

There are at least two possibilities for this growth. The FM domains can percolate within the I2 phase in a manner previously suggested for the percolation of metallic domains within the CO matrix. Alternatively, the I2 phase can become a ferromagnetic metal in a more or less uniform manner, possibly with some small volume fraction undergoing the transition at lower temperatures due to local variations of lattice strain. The presence of this latter fraction may lead to the formation of the insulating "bottlenecks" in an otherwise conducting secondary phase near T_{MI}. Small fluctuations in these insulating regions would then lead to large changes in the sample resistance. In the both scenarios, the insulator-metal transition would exhibit properties characteristic of the percolative transition, as have indeed been found in a variety of manganite samples [2–5], with arguably the most dramatic manifestation being the colossal fluctuations observed in $1/f$ noise measurements [19,20]. In summary, our data strongly suggest that the insulator-metal transition in our sample is due to the changes that occur within the non-charge-ordered parts of the sample. We would like to note that very recently the existence of the secondary low-temperature insulating phase was reported in $Pr_{0.7}Ca_{0.3}MnO_3$ samples [21]. A detailed crystallographic study and structural refinement are needed to establish whether the I2 phase in our sample and the secondary insulating phase in $Pr_{0.7}Ca_{0.3}MnO_3$ are the same.

It has been recently found that in many cases the CO state in manganite materials is unstable against irradiation with x-rays [9,10] or even with visible light [22]. In particular, in $Pr_{0.7}Ca_{0.3}MnO_3$ x-rays destroy the CO state and convert the material to a conducting state which was conjectured to be ferromagnetic [9]. More recently it has been shown that the photoinduced state in related thin films does indeed possess a substantial magnetic moment [23]. We have also therefore carried out a study of the effects of x-ray irradiation in our samples, in particular with the intention of comparing the x-ray-induced transition with the temperature-induced insulator-metal transition that occurs at T_{MI} in the absence of x-rays.

We find that in our samples the charge ordering is also destroyed by x-ray illumination at low temperatures. Fig. 6 shows the intensity and the scattering vector of the (0, 4.5, 0) superlattice peak versus x-ray exposure time. Note that as the crystal lattice gradually relaxes in the transition process, the position of the (0, 4.5, 0) peak also changes, following the changes in the b lattice constant. A diffraction peak was also found at the (5, 0, 0) position. This peak is present only in the CO state and disappears as the sample is irradiated (insets in Fig. 6). After prolonged x-ray irradiation, the a lattice constant

of the remaining CO domains increases by 0.01% and the b constant decreases by 0.045%.

The x-ray-induced effects are present only at temperatures less than 50 K. In fact, the CO state is recovered on heating the x-ray converted samples above T=60 K, as shown in Fig. 7. The x-ray induced FM state, therefore, is unstable above T=60 K. Similar phenomenology was observed previously in $Pr_{0.7}Ca_{0.3}MnO_3$ samples [9]. We note that the data of Fig. 3 are unaffected by these x-ray effects since we find no such effects at T=50 K and above (on cooling), and the data of Fig. 3 at T=10 K were taken quickly after the sample was cooled from 50 K to 10 K in the absence of x-rays.

Because of the strong electron-lattice coupling in the manganites [24], lattice parameters of the FM state are expected to be different from those of the CO phase. It is therefore not surprising that our samples undergo substantial structural changes when irradiated with x-rays below T$\sim$50 K. Fig. 8 shows longitudinal scans (parallel to the scattering vector) in the vicinity of the (0, 4, 0) allowed Bragg peak at T=10 K after various x-ray exposures. The scans were collected using an attenuated beam, so that the x-ray-induced change during the course of a single measurement was negligible. The data of Fig. 8 show that lattice constants of the x-ray-induced phase differ substantially from those of the non-irradiated material. We have tried fitting these data assuming the presence of several phases with fixed lattice constants, but the best fits were obtained when the lattice parameters of the phases were allowed to vary. Such behavior could be the result of a gradual relaxation of the lattice strain exerted by the CO phase on the x-ray-induced phase as the latter phase grows within the CO matrix.

There appears to be a difference between the thermally-induced insulator-metal transition at T_{MI} in the absence of x-rays and the x-ray-induced transition at low temperatures. In the former case, the CO phase is not affected in any measurable manner, while in the latter the conductivity increases simultaneously with the destruction of the CO phase in the related samples [9], and therefore the CO phase is almost certainly converted into the metallic state in the process. Other evidence that the two transitions have different mechanisms comes from the observation that when the samples of a composition similar to ours are irradiated with x-rays *above* T_{MI}, the changes in the intensity of the CO peaks are minimal or even absent [3] while an insulator-metal transition still takes place. Thus, it appears that while a phase distinct from both the FM and the CO phases is required to explain the transition at the relatively high transition temperature T_{MI}, the *low-temperature* x-ray-induced transition may involve only two phases. It would be very interesting to check if this statement holds for other external perturbations, such as magnetic field, for example.

Finally, we briefly discuss samples of different compositions. The exact sample composition depends on the nominal composition of the sample feed rod and on the preparation conditions. Extensive studies on how the properties of ceramic samples of $La_{5/8-y}Pr_yCa_{3/8}MnO_3$ change with composition can be found in Refs. [2,4]. We have investigated several samples with nominal $y \approx 0.35$, all of which exhibited the insulator-metal transition at low temperatures. The magnitude of the resistivity drop at this transition, as well as the low-temperature fraction of the FM phase determined as described above, were different in different samples. Fig. 9 shows temperature dependences of the (0, 5.5, 0) peak intensity and the electric resistance in one of these samples. The low-temperature volume fraction of the FM phase determined from magnetization measurements was only 2.5%. Nevertheless, the sample resistance dropped by more than 2 orders of magnitude on cooling from 100 K to 50 K. The temperature-dependent behavior of the CO phase is perfectly conventional, that is, the intensities and correlation lengths of the charge and orbital ordering saturate at low temperatures and no anomalies are found in the vicinity of T_{MI}. Therefore, the conducting phase in this particular sample must be of a highly filamentary character. Otherwise, a conducting path could not form because of the small fraction of the conducting phase in this sample.

It is natural to assume that local strains associated with twin-domain boundaries and other kinds of structural defects can significantly change electronic properties of the nearby regions due to the strong electron-lattice coupling [24]. The filamentary FM regions that would be induced by such extended lattice defects might appear to be a plausible explanation for the reduced low-temperature resistivity in our samples which have a small low-temperature fraction of the FM phase. The important conclusion that can be drawn from this is that electronic properties of manganites samples can, in some cases, be strongly affected by extremely small amounts of a secondary phase that can arise naturally due to structural defects. Great care in choosing sample growth conditions and sample preparation methods should, therefore, be taken in order to study the properties of the "pure" phases.

IV. CONCLUSIONS

In conclusion, we find that the simple percolation model of the insulator-metal transition in $La_{5/8-y}Pr_yCa_{3/8}MnO_3$ needs to be modified. Our data are inconsistent with the growth of the FM state at the expense of the CO state at low temperatures, at least not in the amounts suggested by the magnetization measurements. We propose that parts of the sample, while insulating, do not exhibit charge ordering below T_{CO} and that the insulator-metal transition is due to the growth of ferromagnetic metallic domains within these parts. Whether these metallic domains actually percolate at

T_{MI}, or more complex structures containing insulating "bottlenecks" are realized in the vicinity of T_{MI} will be the subject of future work. We emphasize that whatever is the actual mechanism responsible for the insulator-metal transition, the CO phase appears to play a less important role in it.

X-ray irradiation at low temperatures destroys the CO state and converts the material to a state which was previously found to be metallic in similar samples. It appears that the mechanism for this low-temperature transition does not require the presence of the phase distinct from both the FM and the CO phases. On the other hand, it has been shown that x-rays do not strongly affect the CO state above T_{MI} while still converting the material to the metallic state [3]. Thus, it is possible that the insulator metal transition at the relatively high temperature T_{MI} and the low-temperature photoinduced transition have different microscopic mechanisms.

We also showed that the insulator-metal transition takes place in samples with an extremely small low-temperature fraction of the FM phase. The conducting phase in these samples must be of a highly filamentary character. We propose that lattice defects and associated strains play an important role in these samples.

We are grateful to M. E. Gershenson, A. J. Millis, and D. Gibbs for important discussions. This work was supported by the NSF under Grant No. DMR-9802513, and by Rutgers University. Work at Brookhaven National Laboratory was carried out under contract No. DE-AC02-98CH10886, US Department of Energy.

---

[1] For a review, see *Colossal Magnetoresistance, Charge Ordering, and related Properties of Manganese Oxides*, edited by C. N. R. Rao and B. Raveau (World Scientific, Singapore, 1998); *Physics of Manganites*, edited by T. A. Kaplan and S. D. Mahanti (Kluwer Academic / Plenum Publishers, New York, 1999); *Colossal Magnetoresistance Oxides*, edited by Y. Tokura (Gordon & Breach, London, 1999)

[2] M. Uehara, S. Mori, C. H. Chen, S-W. Cheong, Nature (London) **399**, 560 (1999)

[3] D. Casa, V. Kiryukhin, O. A. Saleh, B. Keimer, J. P. Hill, Y. Tomioka, Y. Tokura, Europhys. Lett. **47**, 90 (1999)

[4] K. H. Kim, M. Uehara, C. Hess, P. A. Sharma, S-W. Cheong, Phys. Rev. Lett. **84**, 2961 (2000)

[5] N. A. Babushkina, L. M Belova, D. I. Khomskii, K. I. Kugel, O. Yu. Gorbenko, A. R. Kaul, Phys. Rev. B **59**, 6994 (1999)

[6] S. Yunoki, J. Hu, A. L. Malvezzi, A. Moreo, N. Furukawa, E. Dagotto, Phys. Rev. Lett. **80**, 845 (1998); M. Y. Kagan, D. I. Khomskii, M. V. Mostovoy, Europ. Phys. J. B **12**, 217 (1999); E. L. Nagayev, Phys. Status Solidi B **186**, 9 (1994)

[7] P. B. Littlewood, Nature (London) **399**, 529 (1999)

[8] A. Moreo, M. Mayr, A. Feiguin, S. Yunoki, E. Dagotto, Phys. Rev. Lett. **84**, 5568 (2000)

[9] V. Kiryukhin, D. Casa, J. P. Hill, B. Keimer, A. Vigliante, Y. Tomioka, Y. Tokura, Nature (London) **386**, 813 (1997)

[10] V. Kiryukhin, Y. J. Wang, F. C. Chou, M. A. Kastner, R. J. Birgeneau, Phys. Rev. B **59**, R6581 (1999)

[11] D. E. Cox, P. G. Radaelli, M. Marezio, S-W. Cheong, Phys. Rev. B **57**, 3305 (1998)

[12] I. K. Moon, D. H. Jung, K. -B. Lee, Y. H. Jeong, Appl. Phys. Lett. **76**, 2451 (2000)

[13] M. v. Zimmermann, J. P. Hill, Doon Gibbs, M. Blume, D. Casa, B. Keimer, Y. Murakami, Y. Tomioka, Y. Tokura, Phys. Rev. Lett. **83**, 4872 (1999)

[14] Note that in Fig. 3(a) the peak intensity is shown, not the integrated intensity. The data of Fig 3(b) indicate that the integrated intensity plot would give a more conventional "order parameter" curve with a rapid increase in the vicinity of T_{CO} and a slower variation at low temperatures.

[15] C. H. Chen, S. Mori, S-W. Cheong, Phys. Rev. Lett. **83**, 4792 (1999); S. Shimomura, N. Wakabayashi, H. Kuwahara, Y. Tokura, Phys. Rev. Lett. **83**, 4389 (1999); L. Vasiliu-Doloc, S. Rosenkranz, R. Osborn, S. K. Sinha, J. W. Lynn, J. Mesot, O. H. Seeck, G. Preosti, A. J. Fedro, J. F. Mitchell, Phys. Rev. Lett. **83**, 4393 (1999)

[16] Y. Tomioka, A. Asamitsu, H. Kuwahara, Y. Moritomo, Y. Tokura, Phys. Rev. B **53**, R1689 (1996)

[17] The small difference between the CO transition temperatures determined from the diffraction and the specific heat measurements is probably due to the temperature broadening of the CO transition. Note that there is no true divergence of the orbital correlation length at T_{CO} and therefore this temperature is not well defined. Another possible reason for the observed discrepancy is a small miscalibration in the temperature measurement.

[18] S. H. Park, Y. H. Jeong, K. -B. Lee, S. J. Kwon, Phys. Rev. B **56**, 67 (1997)

[19] V. Podzorov, M. Uehara, M. E. Gershenson, T. Y. Koo, S-W. Cheong, Phys. Rev. B **61**, R3784 (2000)

[20] B. Raquet, A. Anane, S. Wirth, P. Xiong, S. von Molnar, Phys. Rev. Lett. **84**, 4485 (2000)

[21] P. G. Radaelli, R. M. Ibberson, D. N. Argyriou, H. Casalta, K. H. Andersen, S-W. Cheong, J. F. Mitchell, preprint cond-mat/0006190.

[22] K. Miyano, T. Tanaka, Y. Tomioka, Y. Tokura, Phys. Rev. Lett. **78**, 4257 (1997)

[23] M. Baran, S. L. Gnatchenko, O. Yu. Gorbenko, A. R. Kaul, R. Szymczak, H. Szymczak, Phys. Rev. B **60**, 9244 (1999)

[24] A. J. Millis, P. B. Littlewood, B. I. Shraiman, Phys. Rev. Lett. **74**, 5144 (1995); A. J. Millis, B. I. Shraiman, R. Mueller, *ibid.* **77**, 175 (1996)

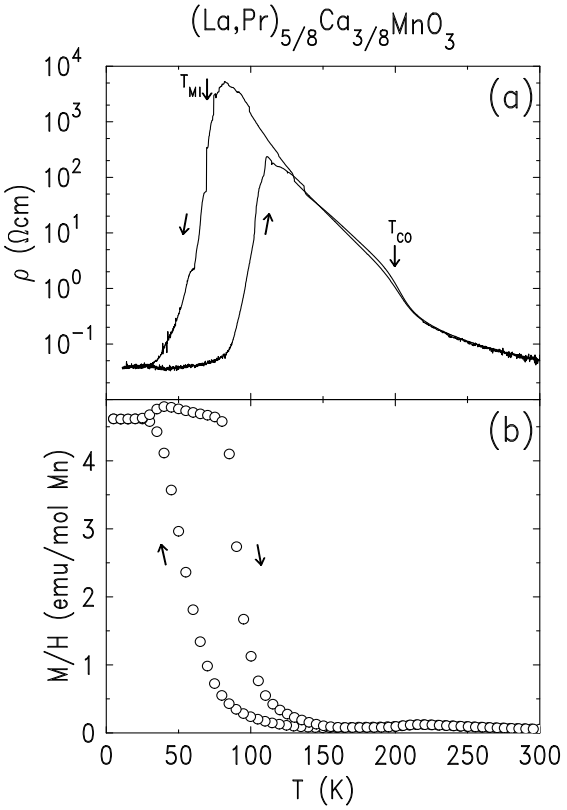

FIG. 1. Temperature dependences of (a) zero-field electric resistivity and (b) the magnetic susceptibility in a 100 Oe magnetic field, taken on heating and on cooling. The transition temperatures T_{CO} and T_{MI} were determined from the maxima in the temperature derivative of the logarithmic resistivity on cooling.

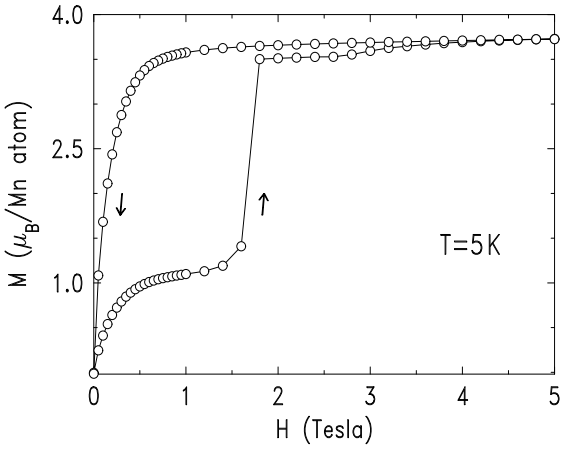

FIG. 2. Magnetization versus magnetic field in ZFC sample taken on ramping the field up and down at T=5 K.

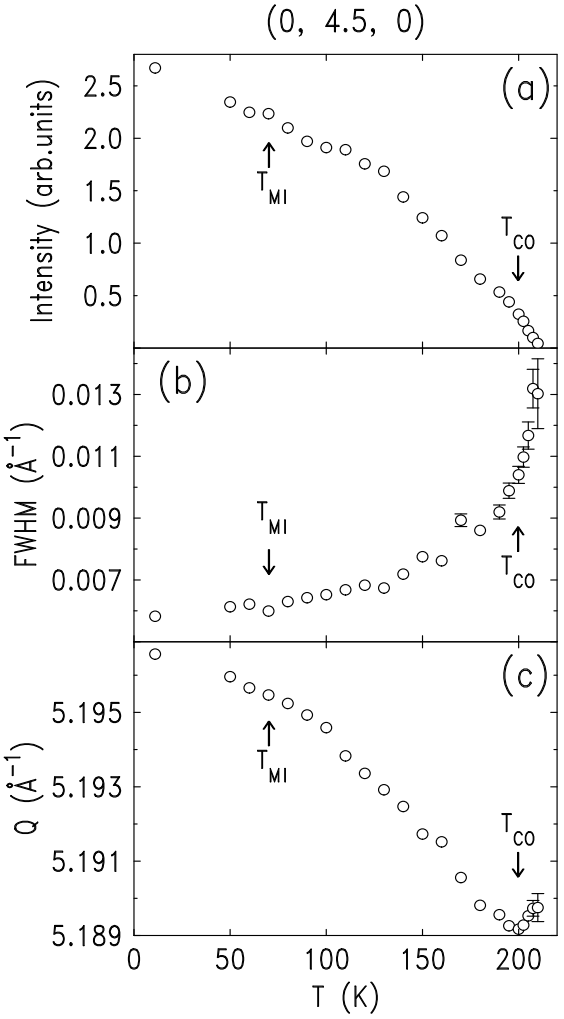

FIG. 3. Temperature dependences of (a) intensity, (b) full width at half maximum, and (c) scattering vector magnitude of the (0, 4.5, 0) superlattice diffraction peak. The data were taken on cooling. The transition temperatures T_{CO} and T_{MI} were determined from the resistivity data of Fig. 1.

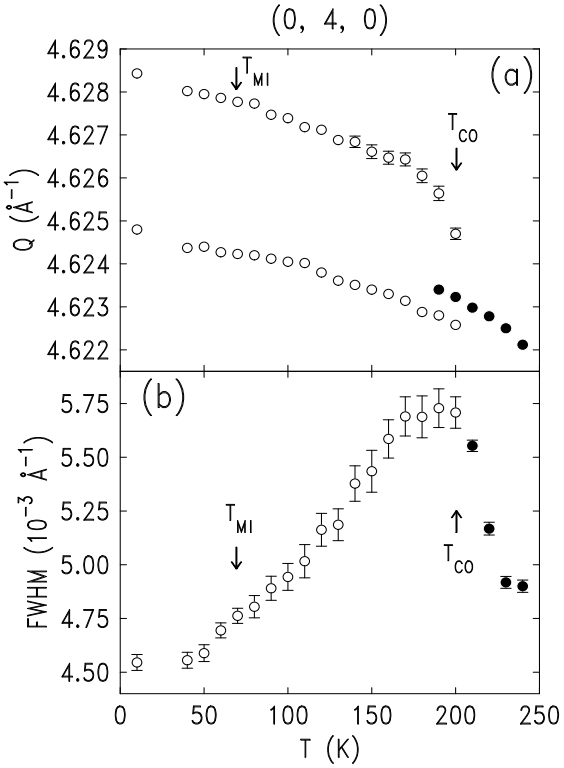

FIG. 4. Temperature dependences of (a) peak positions and (b) full width at half maximum of the Bragg peaks observed in the vicinity of the (0, 4, 0) position in reciprocal space. The data were taken on cooling. The data were fitted to either a single peak (filled circles) or two overlapping peaks (open circles). The transition temperatures T_{CO} and T_{MI} are from the data of Fig. 1.

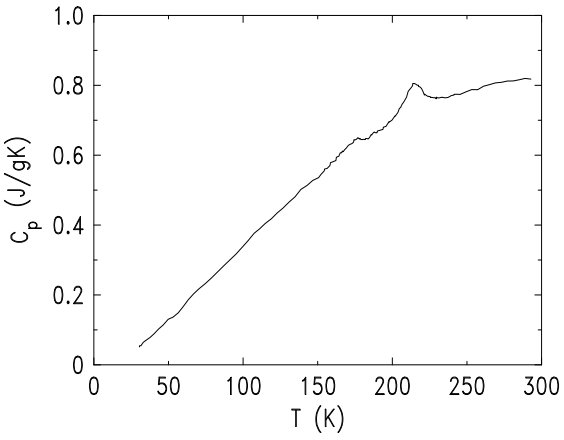

FIG. 5. Temperature dependence of the specific heat.

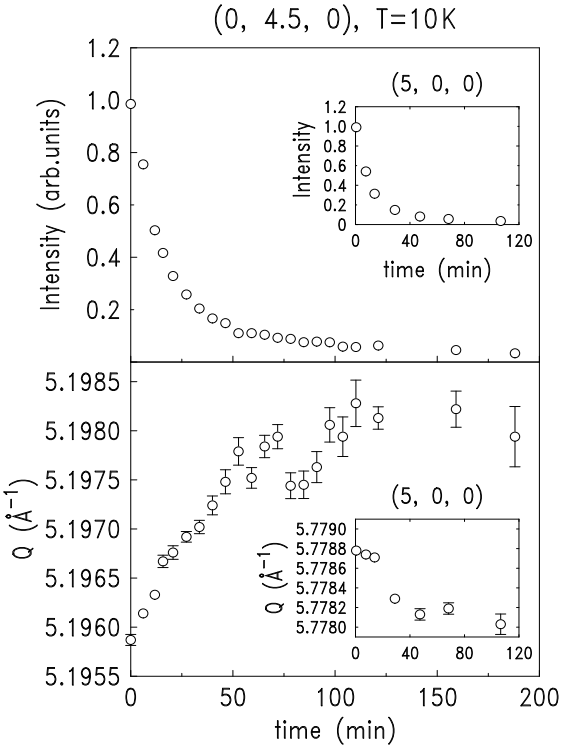

FIG. 6. X-ray exposure dependences of the (0, 4.5, 0) superlattice peak intensity (top panel) and its position (bottom panel) at T=10 K. The insets show the corresponding dependences for the (5, 0, 0) charge-ordering peak.

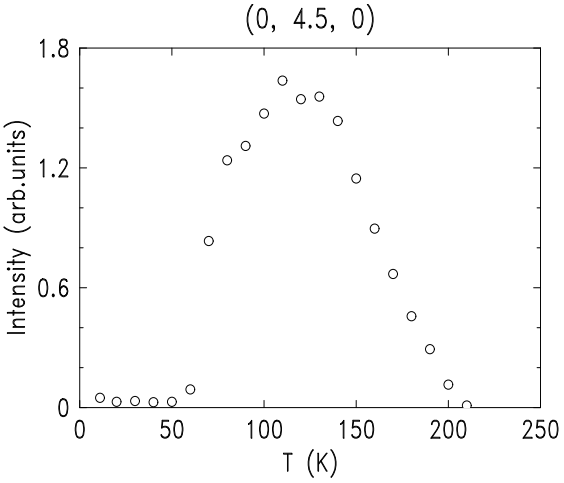

FIG. 7. The intensity of the (0, 4.5, 0) superlattice peak taken on heating from the state in which charge ordering was destroyed by long x-ray exposure.

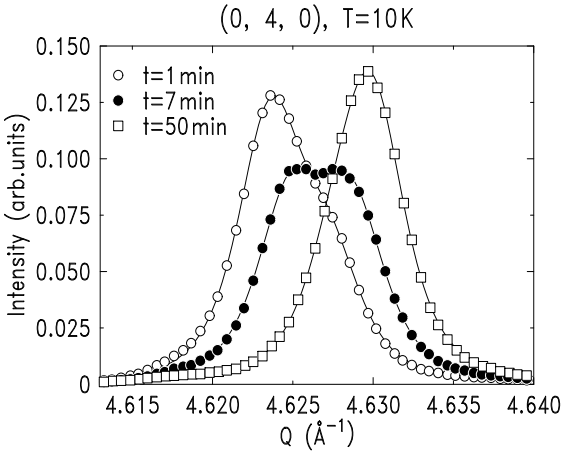

FIG. 8. Longitudinal diffraction scans taken in the vicinity of the (0, 4, 0) position in reciprocal space after various x-ray exposures. The temperature was T=10 K.

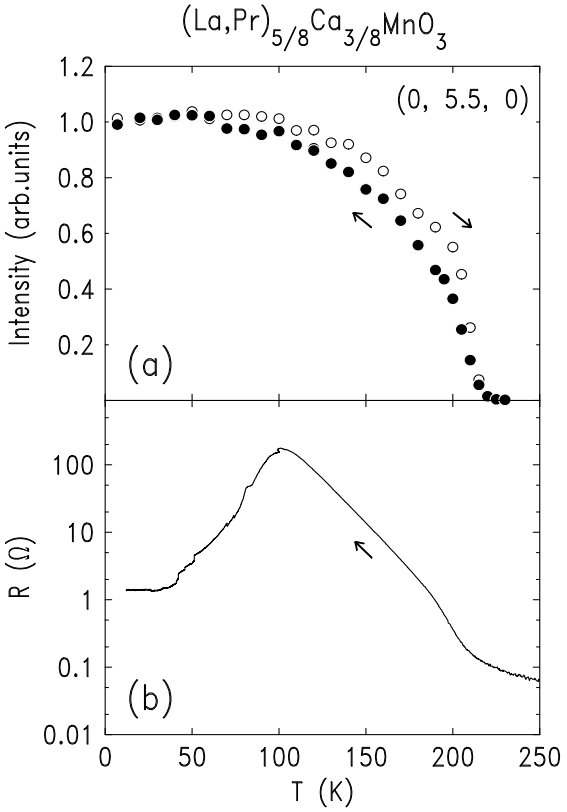

FIG. 9. Temperature dependences of (a) the intensity of the (0, 5.5, 0) superlattice peak, and (b) the electric resistivity in the sample with a small low-temperature fraction of the FM phase.